PROCEEDINGS OF SCIENCE

Conceptual Issues of GPDs

Chueng-Ryong Ji[*†]
North Carolina State University
E-mail: crji@ncsu.edu

Bernard L. G. Bakker
Vrije Universiteit
E-mail: b.l.g.bakker@vu.nl

We discuss the interface between the current theoretical framework based on generalized parton distributions (GPDs) and experimental measurements of deeply virtual Compton scattering (DVCS) observables. We point out that the theoretical framework of GPDs relying on handbag dominance is not sufficient to cover the kinematic region of DVCS experiment with the 12 GeV upgrade at Jefferson Lab. For the general theoretical framework to cover the current and future DVCS experiments, we propose the method of finding the most general hadronic tensor structure with the Lorentz and gauge invariant Compton form factors (CFFs).

QCD Evolution 2017
22-26 May, 2017
Jefferson Lab Newport News, VA - USA

[*]Speaker.
[†]This work was supported in part by the DOE Contract No. DE-FG02-03ER41260.

© Copyright owned by the author(s) under the terms of the Creative Commons Attribution-NonCommercial-NoDerivatives 4.0 International License (CC BY-NC-ND 4.0).

PoS(QCDEV2017)038

1. INTRODUCTION

The investigation of the kinematic issues involving GPDs in DVCS is highly relevant to the 12 GeV upgrade at Jefferson Lab (JLab). Although the value of $Q^2 = -q^2$ (see Fig. 1) for the virtual photon can be twice larger by doubling the energy of the electron from 6 GeV to 12 GeV at JLab, the magnitude of the Mandelstam variable $t = (q - q')^2$ representing the square of the momentum transfer to the target hadron also gets large as Q^2 gets large. This is due to a practical constraint in the set up of the coincidence experiment for DVCS. The ratio of $-t/Q^2$ doesn't get negligible as one might have hoped for the 12 GeV upgrade of JLab. As we pointed out in our review article[1], the present theoretical framework based on the assumption of $-t/Q^2 \ll 1$ needs to be improved in order to cover the kinematic region of virtual Compton scattering experiments. In this work, we review our benchmark calculation with the "bare bone" structure of the DVCS process and discuss the outlook of future developments in the theoretical framework. In Section 2, we use the

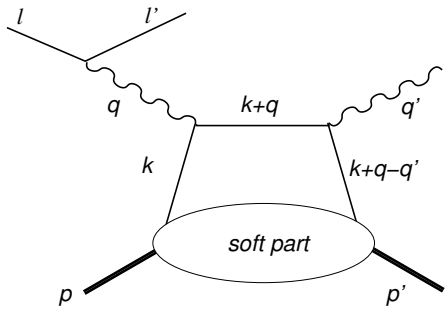

Figure 1: Complete handbag diagram for s-channel Virtual Compton scattering. A quark with momentum k is hit by a virtual photon with momentum q. The final, real photon has momentum q'.

kinematics corresponding to realistic coincidence experiments and focus on the tree-level bare bone amplitudes of DVCS. We discuss how one can see explicit evidence that the original formulation of GPDs is limited to $t = 0$ when the nucleon mass is neglected. This motivates our discussion in Section 3, where we propose the method of finding the most general hadronic tensor structure with the Lorentz and gauge invariant Compton form factors (CFFs). We also discuss two available but not yet well connected high and low energy approaches in this section. Our method towards the generalization of hadronic tensor structures can cover the whole range of kinematics in virtual Compton scattering experiments. Concluding remarks follow in Section 4.

2. Benchmark Calculation in DVCS

This section is devoted to our benchmark calculation of the complete full DVCS amplitude shown in Fig. 2 for the scattering of a massless lepton ℓ off a point-like fermion f of mass m with momentum k. In the final state, we find the scattered lepton ℓ', the fermion f' with momentum k' and a (real) photon γ' with momentum q'. ('Complete' means that the amplitude includes the leptonic part and 'full' means that no approximations are made in the calculation of the hadronic amplitude.) We discuss this simplest possible setting, namely DVCS on a structure-less spin-1/2 particle. Since this provides the bare bone structure on top of which the GPDs are formulated, we

PoS(QCDEV2017)038

think important lessons can be learnt from the analysis of this simplest structure. Kinematic issues revealed in this analysis are expected to prevail in realistic physical situations.

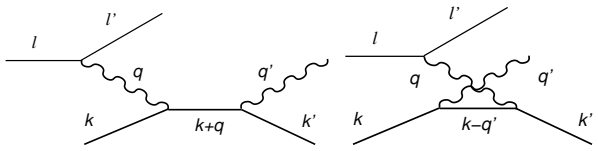

Figure 2: Tree-level diagrams for s-channel and u-channel Compton Scattering

The complete amplitude at tree level can be written as

$$\mathscr{M} = \sum_h \mathscr{L}(\{\lambda',\lambda\}h)\frac{1}{q^2}\mathscr{H}(\{s',s\}\{h',h\}), \tag{2.1}$$

where the quantities λ', λ, h', h, s', and s are the helicities of the outgoing and incoming leptons, outgoing and incoming photons, and the rescattered and target fermions, respectively. Leaving out inessential factors, we may write (see Fig. 2)

$$\begin{aligned}\mathscr{L}(\{\lambda',\lambda\}h) &= \bar{u}(\ell';\lambda')\not{\varepsilon}^*(q;h)u(\ell;\lambda),\\ \mathscr{H}(\{s',s\}\{h',h\}) &= \bar{u}(k';s')(\mathscr{O}_s+\mathscr{O}_u)u(k;s),\end{aligned} \tag{2.2}$$

where the s- and u-channel operators of the intermediate fermion are given by

$$\begin{aligned}\mathscr{O}_s &= \frac{\not{\varepsilon}^*(q';h')(\not{k}+\not{q}+m)\not{\varepsilon}(q;h)}{(k+q)^2-m^2},\\ \mathscr{O}_u &= \frac{\not{\varepsilon}(q;h)(\not{k}-\not{q}'+m)\not{\varepsilon}^*(q';h')}{(k-q')^2-m^2}.\end{aligned} \tag{2.3}$$

The reduced hadronic operators used in the formulation of GPDs are defined as the limits $Q\to\infty$ of the operators given in Eq. (2.3) and found to be

$$\begin{aligned}\mathscr{O}_s|_{\rm Red} &= \frac{\not{\varepsilon}^*(q';h')\gamma^+\not{\varepsilon}(q;h)}{2p^+}\,\frac{1}{x-\zeta},\\ \mathscr{O}_u|_{\rm Red} &= \frac{\not{\varepsilon}(q;h)\gamma^+\not{\varepsilon}^*(q';h')}{2p^+}\,\frac{1}{x},\end{aligned} \tag{2.4}$$

where p^+ is the plus-component of the momentum of the parent hadron target, $x=k^+/p^+$ is the fraction of the plus-component of the momentum carried by the probed quark and $\zeta=(p-p')^+/p^+$ is the "skewness" parameter.

For simplicity, we set the mass m to 0, which is justified by the fact that the dominant energy scale is Q, defined by the square of the momentum of the virtual photon: $Q^2=-q^2$, being much larger than the mass of the particles.

The following kinematics corresponds to the realistic situation where the physical limitations on the detector settings for the coincidence experiment force the outgoing hadrons to be detected

PoS(QCDEV2017)038

off the hard-scattering axis. Usually, the z-axis is chosen along the direction of the hard virtual photon, while the x-axis is chosen along the perpendicular component of the outgoing hadron:

$$\begin{aligned} q^\mu &= \left(-\zeta p^+, 0, 0, \frac{Q^2}{2\zeta p^+}\right), \\ q'^\mu &= \left(\alpha \frac{\Delta^2}{Q^2} p^+, -\Delta, 0, \frac{Q^2}{2\alpha p^+}\right), \\ k^\mu &= \left(x p^+, 0, 0, 0\right), \\ \alpha &= \frac{(x-\zeta)Q^2}{2\Delta^2}\left(1 - \sqrt{1 - \frac{4\zeta\Delta^2}{(x-\zeta)Q^2}}\right), \end{aligned} \tag{2.5}$$

where $k'^\mu = k^\mu + q^\mu - q'^\mu$ and the lepton kinematics is determined by the fact that the leptons produce the virtual photon with a momentum given by the expression for q^μ. Here, the quantity α reduces to ζ in the limit $\Delta/Q \to 0$. In this limit, the kinematics becomes collinear and completely coincides with the special set of coordinates used in Ref. [2]. In order to simplify the results for the amplitudes in this kinematics, we define the quantities

$$D = \frac{4\zeta\Delta^2}{(x-\zeta)Q^2}, \quad D_\pm = 1 \pm \sqrt{1-D}. \tag{2.6}$$

Because $D_+ D_- = D$, we may simplify $1/D_-$ to D_+/D when to take the DVCS limit $Q \to \infty$. Using these notations, we may express α in Eq. (2.5) as $\alpha = 2\zeta D_-/D = 2\zeta/D_+$. The Mandelstam variables are given by

$$s = \frac{(x-\zeta)Q^2}{\zeta}, t = -\frac{2x\Delta^2}{(x-\zeta)D_+}, u = -\frac{2x\Delta^2}{(x-\zeta)D_-}, \tag{2.7}$$

where $s+t+u = -Q^2$. In the $\Delta/Q \to 0$ limit, these expressions of course reduce to the ones found in the collinear frame [2] as well as in the kinematics constrained by $q = q' - \zeta p$ [3] which would result in $t = \zeta^2 M^2 > 0$ that cannot be allowed in DVCS unless $t = 0$ is taken by neglecting the target mass M.

2.1 Results of Helicity Amplitudes

For massless particles, helicity flip is not possible, so we may limit the presentations of the amplitudes to equal helicities for the leptons ($\lambda' = \lambda$) and equal helicites for the hadrons ($s' = s$). Not only the amplitudes in helicity basis satisfy the well-known symmetry based on parity conservation but also the angular-momentum conservation can be applied to our calculations to understand the reasons why some amplitudes vanish identically.

In Table 1, the leptonic amplitudes are presented. In the DVCS limit $Q \to \infty$, only the last amplitude $\mathscr{L}(1/2, 1/2, -1)$ survives. The hadronic amplitudes are presented in Table 2. We see immediately that in the limit $\Delta \to 0$, where D_+ becomes 2 while D_- vanishes, these results reduce to the results in collinear kinematics with the helicity swap, $h' \to -h'$, of the outgoing real photon as discussed in Ref. [1] due to the kinematically invariant nature of the light-front helicity. We also note that the contribution from the longitudinal helicity $h = 0$ of the virtual photon is of order Δ/Q

PoS(QCDEV2017)038

Table 1: Leptonic amplitudes for $\lambda' = \lambda = 1/2$.

λ	h	$\mathscr{L}(\lambda,\lambda,h)$
$\frac{1}{2}$	$+1$	$4\sqrt{2}\frac{(\zeta p^+)^4 Q}{Q^4-4(\zeta p^+)^4}$
$\frac{1}{2}$	0	$i4\frac{(\zeta p^+)^2 Q^3}{Q^4-4(\zeta p^+)^4}$
$\frac{1}{2}$	-1	$-\sqrt{2}\frac{Q^5}{Q^4-4(\zeta p^+)^4}$

Table 2: Full and reduced hadronic amplitudes for $s' = s = \pm 1/2$ and $h' = 1$.

s	h	$\mathscr{H}$	$\mathscr{H}_{\rm red}$
$\frac{1}{2}$	$+1$	0	$2\sqrt{2}\sqrt{\frac{x-\zeta}{x}}\frac{1}{\sqrt{D_+}}$
$\frac{1}{2}$	0	0	$4i\frac{\zeta\Delta}{Q\sqrt{x(x-\zeta)D_+}D_+}$
$\frac{1}{2}$	-1	$2\sqrt{2}\sqrt{\frac{x}{x-\zeta}}\frac{1}{\sqrt{D_+}}$	0
$-\frac{1}{2}$	$+1$	$-\sqrt{2}\frac{\zeta}{\sqrt{x(x-\zeta)}}\frac{D_-}{\sqrt{D_+}}$	$\sqrt{2}\sqrt{\frac{x}{x-\zeta}}\sqrt{D_+}$
$-\frac{1}{2}$	0	$-4i\frac{\zeta\Delta}{Q\sqrt{x(x-\zeta)D_+}}$	0
$-\frac{1}{2}$	-1	$\sqrt{2}\sqrt{\frac{x-\zeta}{x}}\sqrt{D_+}$	0

and should not be neglected when computing the amplitude unless the kinematic region is limited to $t = 0$.

In Table 3, complete full and reduced amplitudes are presented without any expansion in orders of Q. The complete full amplitudes are our exact results at tree level without any approximation. As one can see, the difference between the full and reduced results are manifest. To compare the full and reduced results in the DVCS region, we have expanded the complete amplitudes up to order $1/Q^4$ as shown in Table 4. For the leading order in $1/Q$, full and reduced results are in complete agreement with the helicity swap [1], $h' \to -h'$, mentioned above. The difference between the full and reduced results is evident however in the orders $1/Q^3$ and $1/Q^4$. In Table 4, one can see that the deviation occurs in the orders Δ^2/Q^2 as well as $\Delta(\zeta p^+)^2/Q^3$. Thus, the reduced formulation for the leading twist (twist 2) GPDs [2, 3] is accurate only at $t = 0$ and starts to deviate from the exact results to the order of $-t/Q^2$ as well as $(\zeta p^+)^2\sqrt{-t}/Q^3$. We note that *e.g.* in JLab the values of $-t/Q^2$ are larger than 5-10% and therefore caution against using the lowest-twist formulas for the analysis of experimental data in situations where the net transverse-momentum transfer to the target is not that small compared to Q.

2.2 Tensor formulation at tree level

We discuss here the hadronic tensor part at tree level, where the GPDs are constants. Rewriting the s- and u- channel hadronic amplitudes defined in Eqs. (2.2) and (2.3) as

$$\begin{aligned}\bar{u}(k';s')\mathscr{O}_s u(k;s) &= \varepsilon_\mu{}^*(q';h')\varepsilon_\nu(q;h)T_s{}^{\mu\nu},\\ \bar{u}(k';s')\mathscr{O}_u u(k;s) &= \varepsilon_\mu{}^*(q';h')\varepsilon_\nu(q;h)T_u{}^{\mu\nu},\end{aligned} \tag{2.8}$$

PoS(QCDEV2017)038

Table 3: Complete full and reduced amplitudes.

λ	h'	s	$\mathscr{A}=\Sigma\mathscr{L}\frac{1}{q^2}\mathscr{H}$	$\mathscr{A}_{\rm red}=\Sigma\mathscr{L}\frac{1}{q^2}\mathscr{H}_{\rm red}$
$\frac{1}{2}$	1	$\frac{1}{2}$	$4\sqrt{\frac{x}{(x-\zeta)D_+}}\frac{Q^3}{Q^4-4(\zeta p^+)^4}$	$-4(\zeta p^+)^2\sqrt{\frac{x-\zeta}{xD_+}}\frac{4Q\Delta(\zeta p^+)^2-D_-Q^4}{\Delta(Q^4-4(\zeta p^+)^4)}$
$\frac{1}{2}$	1	$-\frac{1}{2}$	$2\frac{2Q\{Q^3(x-\zeta)-4\Delta\zeta(\zeta p^+)^2\}-D_-\{Q^4(x-\zeta)-4\zeta(\zeta p^+)^4\}}{\sqrt{x(x-\zeta)D_+}Q(Q^4-4(\zeta p^+)^4)}$	$-8\sqrt{\frac{xD_+}{x-\zeta}}\frac{(\zeta p^+)^4}{Q(Q^4-4(\zeta p^+)^4)}$
$\frac{1}{2}$	-1	$\frac{1}{2}$	$2\frac{4(\zeta p^+)^2\{2Q\Delta\zeta-(\zeta p^+)^2(x-\zeta)D_+\}-D_-Q^4\zeta}{\sqrt{x(x-\zeta)D_+}Q(Q^4-4(\zeta p^+)^4)}$	$2\sqrt{\frac{xD_+}{x-\zeta}}\frac{Q^3}{Q^4-4(\zeta p^+)^4)}$
$\frac{1}{2}$	-1	$-\frac{1}{2}$	$-16\sqrt{\frac{x}{(x-\zeta)D_+}}\frac{(\zeta p^+)^4}{Q(Q^4-4(\zeta p^+)^4)}$	$4\sqrt{\frac{x-\zeta}{xD_+}}\frac{Q^3\Delta-(\zeta p^+)^2D_-Q^2}{\Delta(Q^4-4(\zeta p^+)^4)}$

Table 4: Expanded Complete full and reduced amplitudes up to the order of $1/Q^4$.

λ	h'	s	$\mathscr{A}=\Sigma\mathscr{L}\frac{1}{q^2}\mathscr{H}$	$\mathscr{A}_{\rm red}=\Sigma\mathscr{L}\frac{1}{q^2}\mathscr{H}_{\rm red}$
$\frac{1}{2}$	1	$\frac{1}{2}$	$2\sqrt{2}\sqrt{\frac{x}{x-\zeta}}\frac{1}{Q}\left(1+\frac{\zeta\Delta^2}{2(x-\zeta)Q^2}\right)$	$4\sqrt{2}\frac{\zeta(\zeta p^+)^2\Delta}{\sqrt{x(x-\zeta)}Q^4}$
$\frac{1}{2}$	1	$-\frac{1}{2}$	$2\sqrt{2}\sqrt{\frac{x-\zeta}{x}}\frac{1}{Q}\left(1-\frac{\zeta\Delta^2}{2(x-\zeta)Q^2}-\frac{4\zeta(\zeta p^+)^2\Delta}{(x-\zeta)Q^3}\right)$	0
$\frac{1}{2}$	-1	$\frac{1}{2}$	$2\sqrt{2}\frac{1}{\sqrt{x(x-\zeta)}}\frac{1}{Q}\left(\frac{4\zeta(\zeta p^+)^2\Delta}{Q^3}-\frac{\zeta^2\Delta^2}{(x-\zeta)Q^2}\right)$	$2\sqrt{2}\sqrt{\frac{x}{x-\zeta}}\frac{1}{Q}\left(1-\frac{\zeta\Delta^2}{2(x-\zeta)Q^2}\right)$
$\frac{1}{2}$	-1	$-\frac{1}{2}$	0	$2\sqrt{2}\sqrt{\frac{x-\zeta}{x}}\frac{1}{Q}\left(1+\frac{\zeta\Delta^2}{2(x-\zeta)Q^2}-\frac{2\zeta(\zeta p^+)^2\Delta}{(x-\zeta)Q^3}\right)$

and neglecting the inessential fermion mass m as before, we express the tensorial amplitudes ${T_s}^{\mu\nu}$ and ${T_u}^{\mu\nu}$ as

$$\begin{aligned}{T_s}^{\mu\nu} &= \frac{k_\alpha+q_\alpha}{s}\bar{u}(k';s')\gamma^\mu\gamma^\alpha\gamma^\nu u(k;s),\\ {T_u}^{\mu\nu} &= \frac{k_\alpha-q'_\alpha}{u}\bar{u}(k';s')\gamma^\nu\gamma^\alpha\gamma^\mu u(k;s),\end{aligned}\tag{2.9}$$

respectively. Using the identity

$$\gamma^\mu\gamma^\alpha\gamma^\nu = g^{\mu\alpha}\gamma^\nu+g^{\alpha\nu}\gamma^\mu-g^{\mu\nu}\gamma^\alpha+i\varepsilon^{\mu\alpha\nu\beta}\gamma_\beta\gamma_5\tag{2.10}$$

and the Sudakov variables $n^\mu(+)=(1,0,0,0)$ and $n^\mu(-)=(0,0,0,1)$, one may expand ${T_s}^{\mu\nu}$ and ${T_u}^{\mu\nu}$ to find the terms proportional to $\bar{u}(k';s')\not{n}(-)u(k;s)$ and $\bar{u}(k';s')\not{n}(-)\gamma_5u(k;s)$ that correspond to the nucleon GPDs $H(x,\Delta^2,\xi)$ and $\tilde{H}(x,\Delta^2,\xi)$ defined in the original formulation of GPDs [2, 3], respectively. For example, one finds for T_s in leading order of Q [4]

$$\begin{aligned}{T_s}^{\mu\nu} = \frac{q^-}{s}\Big[&\{n^\mu(-)n^\nu(+)+n^\nu(-)n^\mu(+)-g^{\mu\nu}\}\bar{u}(k';s')\not{n}(-)u(k;s)\\ &-i\varepsilon^{\mu\nu\alpha\beta}n_\alpha(-)n_\beta(+)\bar{u}(k';s')\not{n}(-)\gamma_5u(k;s)\Big],\end{aligned}\tag{2.11}$$

where $q^-\sim Q^2/\zeta p^+$ is the leading order in Q. A similar expression is found for T_u. This expression is equivalent to the one obtained by the reduced operator given by Eq. (2.4) that corresponds to the original formulation of the leading twist GPDs [2, 3]. However, in the kinematics

PoS(QCDEV2017)038

given by Eq. (2.5), we should use ($k^- = 0$ in the massless case) $q^\mu = q^+ n^\mu(+) + q^- n^\mu(-)$, $q'^\mu = q'^+ n^\mu(+) + q'^- n^\mu(-) + q'^\mu_\perp$, $k^\mu = k^+ n^\mu(+)$, $k'^\mu = k'^+ n^\mu(+) + k'^- n^\mu(-) + k'^\mu_\perp$ in Eq. (2.9) to find the corresponding T_s and T_u. It corresponds to the use of full operator given by Eq. (2.3). The point is that one should not retain only the terms proportional to the highest power in Q, namely those proportional to q^-, in the realistic situation of DVCS experiments. As we have shown in Table 3, our exact results of complete tree-level amplitudes including all orders in Q are apparently different from those obtained by the reduced operator. As shown in Table 4, the results from the reduced operator agree with our results only in the leading order terms but not in the Δ^2/Q^2 order and the terms beyond that order. This reveals that the applicabilities of the original formulations of the leading twist GPDs [2, 3] are limited to the $t = \Delta^2 = 0$ kinematic region when the nucleon mass is neglected. We caution against using the $t = 0$ formulas in the analysis of experimental data in situations where Δ is not small compared to Q.

3. Toward Generalized Tensor Structure

The hadronic tensors used in the formulation of GPDs do not yield the higher order corrections of $\sim 1/Q$ correctly even in the bare bone tree-level amplitude. Thus, it will be crucial to find the generalized hadronic tensor structure.

Since the spin degrees of freedom for the nucleon, the virtual photon, and the real photon are given by 2, 3, and 2, respectively, the total independent number of available DVCS amplitudes respecting parity symmetry can be found to be 12. Therefore, in general, twelve GPDs are needed to describe the DVCS amplitudes. The four GPDs discussed in Refs. [2, 3], namely, $H(x,\Delta^2,\xi), E(x,\Delta^2,\xi), \tilde{H}(x,\Delta^2,\xi)$, and $\tilde{E}(x,\Delta^2,\xi)$ are just a subset of the total twelve GPDs. Moreover, the hadronic tensor $T^{\mu\nu}$ for the DVCS amplitudes must have twelve independent basis tensors associated with the 12 GPDs and each associated tensor must be general enough to cover the full kinematic regime of DVCS experiments. For example, the associated tensor structures for the four GPDs ($H(x,\Delta^2,\xi), E(x,\Delta^2,\xi), \tilde{H}(x,\Delta^2,\xi)$, and $\tilde{E}(x,\Delta^2,\xi)$) presented in Refs. [2, 3] must be generalized to cover the kinematic region $t < -|t_{\rm min}| < 0$. According to Ref. [5], $|t_{\rm min}| \approx 0.1({\rm GeV}/c)^2$ was given in the measurement of beam spin asymmetries in the JLab DVCS experiment.

3.1 Two Approaches from Low and High Energies

As far as we can see from the literature, there were two different approaches to find the most general hadronic tensor structures in virtual Compton scattering processes: one from the low energy side [6, 7, 8, 9] and the other from the high energy side [10, 11, 12, 13, 14, 15]. In the 1970s, M. Perrottet[6] and R. Tarrach[7] have started constructing the most general tensor structures focusing more on the low energy Compton scattering issues. They followed the mathematical treatment for expansions of holomorphic spinor amplitudes with coefficients free from kinematical singularities constructed by C. de Calan and R. Stora[8]. Twelve scalar Compton form factors (CFFs) were introduced to analyze the virtual Compton scattering amplitude. This line of approach has been pursued even after the formulation of GPDs emerged[9] without making any connection between CFFs and GPDs. However, after the formulation of GPDs appeared, another approach more recently developed was to go beyond the leading twist formulation of DVCS in terms of GPDs and

PoS(QCDEV2017)038

include the higher twist contributions to extend the formulation in terms of GPDs[12, 13, 14, 15]. While this high energy approach also introduces the same number (twelve) of CFFs, the GPDs introduced in this approach are not yet related to the ones introduced in the low energy approach. In particular, the GPDs in the high energy approach are based on the handbag dominance (see Fig. 1) and the factorization of amplitudes. Although the two approaches could be complementary to each other and in principle one may anticipate to even see the equivalence of the two approaches, the connection between them has not yet been fully established. The expressions given by the two approaches are apparently different for the nucleon target. For example, Tarrach's expression includes the scalar bi-product of spinors, $\bar{u}u$, and the correspondence to the expression for the spin-0 target is manifest, while the expression from the approach of GPDs does not have the component of $\bar{u}u$ but instead has the component of $\bar{u}\gamma_5 u$ which is absent in Tarrach's expression. Nevertheless, it doesn't preclude the equivalence of the two expressions since the Gordon decomposition and its extension for the nucleon state can easily connect the apparently different bi-products. For example, the matrix element of a pseudoscalar can be written in terms of the matrix elements of the axial vector and the tensor operators:

$$(p'-p)^\mu \bar{u}(p')\gamma_5 u(p) = 2M\bar{u}(p')\gamma^\mu\gamma_5 u(p) + i\varepsilon^{\mu\nu\alpha\beta}(p+p')_\nu \bar{u}(p')\sigma_{\alpha\beta}u(p), \tag{3.1}$$

where M is the nucleon mass. Similarly, one can use the following substitutions for the nucleon state:

$$(p+p')_\mu \to 2M\gamma_\mu - i\sigma_{\mu\nu}q^\nu \tag{3.2}$$

and

$$2i\varepsilon_{\mu\nu\alpha\beta}\gamma_5\gamma^\nu p^\alpha p'^\beta \to q^2\gamma_\mu - 2iM\sigma_{\mu\nu}q^\nu. \tag{3.3}$$

Thus, for the case of nucleon form factors, we note that the usual decomposition of $J^\mu = \gamma^\mu F_1(q^2) + i\frac{\sigma_{\mu\nu}q^\nu}{2M}F_2(q^2)$ in terms of vector and tensor currents with the Dirac (F_1) and Pauli (F_2) form factors is just one of the following six possible decompositions [16]:

$$\begin{aligned}
J^\mu &= \gamma^\mu F_1 + i\frac{\sigma^{\mu\nu}q_\nu}{2M}F_2 \\
&= \gamma^\mu(F_1+F_2) - \frac{(p+p')^\mu}{2M}F_2 \\
&= \frac{(p+p')^\mu}{2M}\frac{4M^2F_1+q^2F_2}{4M^2-q^2} - i\varepsilon^{\mu\nu\alpha\beta}\gamma_5\gamma_\nu p_\alpha p'_\beta\frac{2(F_1+F_2)}{4M^2-q^2} \\
&= \frac{(p+p')^\mu}{2M}F_1 + i\frac{\sigma^{\mu\nu}q_\nu}{2M}(F_1+F_2) \\
&= \gamma^\mu(F_1+\frac{q^2}{4M^2}F_2) - i\varepsilon^{\mu\nu\alpha\beta}\gamma_5\gamma_\nu p_\alpha p'_\beta\frac{F_2}{2M^2} \\
&= i\frac{\sigma^{\mu\nu}q_\nu}{2M}(\frac{4M^2}{q^2}F_1+F_2) + i\varepsilon^{\mu\nu\alpha\beta}\gamma_5\gamma_\nu p_\alpha p'_\beta\frac{2F_1}{q^2},
\end{aligned} \tag{3.4}$$

where the equivalence meant the equality on the level of matrix elements, *e.g.* $\bar{u}J^\mu u$, but not on the level of operators themselves. For the nucleon target, these six different decompositions in Eq. (3.4) are all equivalent. Any particular choice of decomposition may depend on a matter of convenience and/or effectiveness in the given situation of computation. Therefore, one should

PoS(QCDEV2017)038

look into the commonality of the two approaches as well as the differences between them in order to make progress towards the settlement of the most general hadronic tensor structures in DVCS which can cover the entire kinematic regime of current and future experimental facilities.

3.2 DNA Method

Here we propose a method that is free of poles *ab inito* so that no regularisation is necessary. We focus on the spin-0 hadron target as an explicit example. Defining

$$d^{\mu\nu\alpha\beta} = g^{\mu\nu}g^{\alpha\beta} - g^{\mu\beta}g^{\nu\alpha}, \tag{3.5}$$

we find that $d^{\mu\nu\alpha\beta}$ serves as the back bone of the Compton tensor. To this back bone, pairs of momenta are fixed by contraction, like the base pairs in DNA. We note that $d^{\mu\nu\alpha\beta}$ is symmetric under the simultaneous interchange $\mu \leftrightarrow \nu$, $\alpha \leftrightarrow \beta$ and changes sign by the interchanges $\mu \leftrightarrow \alpha$, and $\nu \leftrightarrow \beta$. Using this back bone we construct pieces of "DNA" by contracting it with the three basis four vectors. With an obvious notation we write them as follows:

$$\begin{aligned}
G^{\mu\nu}(q'q) &= q'_\alpha d^{\mu\nu\alpha\beta} q_\beta = q'\cdot q\, g^{\mu\nu} - q^\mu q'^\nu,\\
G^{\mu\nu}(qq) &= q_\alpha d^{\mu\nu\alpha\beta} q_\beta = q^2\, g^{\mu\nu} - q^\mu q^\nu,\\
G^{\mu\nu}(q'q') &= q'_\alpha d^{\mu\nu\alpha\beta} q'_\beta = q'^2\, g^{\mu\nu} - q'^\mu q'^\nu,\\
G^{\mu\nu}(\overline{P}q) &= \overline{P}_\alpha d^{\mu\nu\alpha\beta} q_\beta = \overline{P}\cdot q\, g^{\mu\nu} - q^\mu \overline{P}^\nu,\\
G^{\mu\nu}(q'\overline{P}) &= q'_\alpha d^{\mu\nu\alpha\beta} \overline{P}_\beta = \overline{P}\cdot q'\, g^{\mu\nu} - \overline{P}^\mu q'^\nu.
\end{aligned} \tag{3.6}$$

The first tensor is identical with $q'\cdot q$ times Tarrach's projector, the second and the third ones are multiples of the projectors used by Perrottet. The last two are novel. Including $\overline{P}$ in the set of building blocks of projectors, more freedom in the construction of the transverse tensor is created. These five tensors have vanishing contractions with q'_μ and q_ν and are free of kinematical singularities *ab initio*. The latter property obviates the necessity of the Tarrach construction to remove the single and double poles. Given these building blocks the transverse tensor $\tilde{T}^{\mu\nu}_{DNA} := \sum_{i=1}^{5} \mathscr{S}_i \tilde{T}^{(i)\mu\nu}_{\rm DNA}$ can be written as follows

$$\begin{aligned}
\tilde{T}^{\mu\nu}_{\rm DNA} &= \mathscr{S}_1\, G^{\mu\nu}(q'q)\\
&+ \mathscr{S}_2\, G^{\mu\lambda}(q'q')\, G_\lambda{}^\nu(qq)\\
&+ \mathscr{S}_3\, G^{\mu\lambda}(q'\overline{P})\, G_\lambda{}^\nu(\overline{P}q)\\
&+ \mathscr{S}_4\, [G^{\mu\lambda}(q'\overline{P})\, G_\lambda{}^\nu(qq) + G^{\mu\lambda}(q'q')\, G_\lambda{}^\nu(\overline{P}q)]\\
&+ \mathscr{S}_5\, G^{\mu\lambda}(q'q')\overline{P}_\lambda \overline{P}_{\lambda'} G^{\lambda'\nu}(qq).
\end{aligned} \tag{3.7}$$

By direct computation one may check that the DNA representation is simply related to Metz's thesis [17] as given in the following equation:

$$\begin{aligned}
M_1^{\mu\nu} &= -q'\cdot q\, g^{\mu\nu} + q^\mu q'^\nu,\\
M_2^{\mu\nu} &= -(\bar{P}\cdot q)^2\, g^{\mu\nu} - q'\cdot q\, \bar{P}^\mu \bar{P}^\nu + \bar{P}\cdot q\,(\bar{P}^\mu q'^\nu + q^\mu \bar{P}^\nu),\\
M_3^{\mu\nu} &= q'^2 q^2\, g^{\mu\nu} + q'\cdot q\, q'^\mu q^\nu - q^2 q'^\mu q'^\nu - q'^2 q^\mu q^\nu,\\
M_4^{\mu\nu} &= \bar{P}\cdot q\,(q'^2 + q^2)\, g^{\mu\nu} - \bar{P}\cdot q\,(q'^\mu q'^\nu + q^\mu q^\nu)\\
&\quad -q^2 \bar{P}^\mu q'^\nu - q'^2 q^\mu \bar{P}^\nu + q'\cdot q\,(\bar{P}^\mu q^\nu + q'^\mu \bar{P}^\nu),\\
M_{19}^{\mu\nu} &= (\bar{P}\cdot q)^2 q'^\mu q^\nu + q'^2 q^2 \bar{P}^\mu \bar{P}^\nu - \bar{P}\cdot q\, q^2 q'^\mu \bar{P}^\nu - \bar{P}\cdot q\, q'^2 \bar{P}^\mu q^\nu.
\end{aligned} \tag{3.8}$$

PoS(QCDEV2017)038

(For historical reasons, the fifth tensor has subscript 19.). We get

$$\tilde{T}^{(1)}_{\rm DNA} = -M_1, \quad \tilde{T}^{(2)}_{\rm DNA} = M_3, \quad \tilde{T}^{(3)}_{\rm DNA} = -M_2, \quad \tilde{T}^{(4)}_{\rm DNA} = M_4, \quad \tilde{T}^{(5)}_{\rm DNA} = M_{19}. \tag{3.9}$$

The tensor M_{19} does not fit immediately in the Bardeen-Tung construction, but was introduced in Ref. [18] as $T_{19} \equiv M_{19}/q' \cdot q$ together with two other ones that can only occur for spin-1/2 targets, in order to create more freedom to construct the Compton tensor. Metz used this tensor to replace another one in his original transverse basis. We shall not discuss this matter in more detail, but just note that in the DNA construction this tensor occurs quite naturally.

A final remark is in order here. In the literature sometimes one sees representations of the Compton tensor that are not manifestly transverse. In those cases use has been made of the equations of motion for the wave functions of the external particles, hadrons and photons. Such a representation has the disadvantage that because terms have been omitted, a check of the original equation is not possible anymore.

4. CONCLUSIONS

We find that the original formulation [2, 3] of DVCS in terms of GPDs are not satisfactory unless the kinematic region for the coincidence experiment is limited to $t = 0$. The determination of all independent structures is important for the analysis of DVCS data anticipated from the 12 GeV upgrade of JLab. In particular, maintaining electromagnetic gauge invariance is an important constraint to obtain the general tensor structure of DVCS ampltiudes. Both high and low energy approaches for the effective hadronic tensor need to be further investigated to pin down whether their general tensor structures are indeed equivalent or not. For the general theoretical framework to cover the current and future DVCS experiments, we proposed the DNA method of finding the most general hadronic tensor structure with the Lorentz and gauge invariant Compton form factors (CFFs).

References

[1] C.-R. Ji and B. L. G. Bakker, Int. J. Mod. Phys. E **22**, 1330002 (2013).

[2] X. D. Ji, Phys. Rev. Lett. **78**, 610 (1997); Phys. Rev. D **55**, 7114 (1997).

[3] A. V. Radyushkin, Phys. Lett. B **380**, 417 (1996), Phys. Rev. D **56**, 5524 (1997).

[4] B.L.G.Bakker and C.-R.Ji, Phys. Rev. D **83**, 091502(R) (2011).

[5] G. Gavalian et. al. (CLAS Collaboration), Phys. Rev. C **80**, 035206 (2009).

[6] M. Perrottet, Lett. Nuovo Cim. **7**, 915 (1973).

[7] R. Tarrach, Nuovo Cim. **28 A**, 409 (1975).

[8] C. de Calan and R. Stora, *Decomposition of Holomorphic Spinor Amplitudes*, CERN Ref. TH. 1004 (1969).

[9] D. Drechsel, G. Knöchlein, A.Yu. Korchin, A. Metz, and S. Scherer, Phys. Rev. C **57**, 941 (1998).

[10] N. Kivel, M. V. Polyakov and M. Vanderhaeghen, Phys. Rev. D **63**, 114014 (2001).

PoS(QCDEV2017)038

[11] A. Freund and M. McDermott, Eur. Phys. J. C **23**, 651 (2002).

[12] A. V. Belitsky and D. Müller, Nucl.Phys. B**589**, 611 (2000).

[13] A.V. Belitsky, D. Müller, and A. Kirchner, Nucl. Phys. B **629**, 323 (2002).

[14] A. V. Belitsky and D. Müller, Phys. Rev. D **79**, 014017 (2009).

[15] A. V. Belitsky and D. Müller, Phys. Rev. D **82**, 074010 (2010), arXiv:1005.5209.

[16] B.L.G.Bakker and C.-R.Ji, Few-Body Syst **58**, 1 (2017).

[17] Metz, M.: *Virtuelle Comptonstreuung und die Polarisierbarkeiten des Nukleons* (in German), PhD thesis, Universität Mainz, 1997.

[18] Bardeen, W. A. and Tung, Wu-Ki: Invariant Amplitudes for Photon Processes, Phys. Rev. **173**, 1423 (1968).

PoS(QCDEV2017)038